Modeling and Control of a New Quadrotor Manipulation System

Ahmed Khalifa[1], Mohamed Fanni[2], Ahmed Ramadan[3], Ahmed Abo-Ismail[4]

[1,4] Mechatronics and Robotics Engineering Dept., School of Innovative Design Engineering, Egypt-Japan University of Science and Technology, New Borg-El-Arab city, Alexandria, Egypt
ahmed.khalifa@ejust.edu.eg , aboismail@ejust.edu.eg
[2] Prod. Eng. & Mechanical Design Dept., Faculty of Engineering, Mansoura University, Mansoura, Egypt
mfanni@mans.edu.eg
[3] Computer & Automatic Control Dept., Faculty of Engineering, Tanta University, Tanta, Egypt
ahmed.ramadan@ejust.edu.eg

Abstract— **This paper introduces a new quadrotor manipulation system that consists of a 2-link manipulator attached to the bottom of a quadrotor. This new system presents a solution for the drawbacks found in the current quadrotor manipulation system which uses a gripper fixed to a quadrotor. Unlike the current system, the proposed system enables the end-effector to achieve any arbitrary orientation and thus increases its degrees of freedom from 4 to 6. Also, it provides enough distance between the quadrotor and the object to be manipulated. This is useful in some applications such as demining applications. System kinematics and dynamics are derived which are highly nonlinear. Controller is designed based on feedback linearization to track desired trajectories. Controlling the movements in the horizontal directions is simplified by utilizing the derived nonholonmic constraints. Finally, the proposed system is simulated using MATLAB/SIMULINK program. The simulation results show the effectiveness of the proposed controller.**

Keywords- Aerial manipulation; Quadrotor;2-link manipulator; Feedback linearization; Demining devices

I. INTRODUCTION

In recent years, extensive research works on unmanned aerial vehicles (UAVs) has been done [2, 3, 4, 6, 7]. UAVs offer possibilities of speed and access to regions that are otherwise inaccessible to ground robotic vehicles. Quadrotor vehicles possess certain essential characteristics, which highlight their potential for use in search and rescue applications. Characteristics that provide a clear advantage over other flying UAVs include their Vertical Take Off and Landing (VTOL) and hovering capability, as well as their ability to make slow precise movements. There are also clear advantages to have a four rotor based propulsion system, such as a higher payload capacity, and impressive maneuverability, particularly in traversing through an environment with many obstacles, or landing in small areas.

The design and control for aerial grasping was presented in [1]. By allowing UAVs, specifically quadrotors, to interact with the environment, one can get an entire new set of applications. First, allowing robots to fly and perch on rods or beams allow them to increase the endurance of their missions (e.g. For its battery charging). Second, the ability to grasp and manipulate objects allows robots to access payloads that are unavailable to ground robots. Also, there are fewer workspace constraints for aerial robots. With this quadrotor system, we produce a 4-DOF manipulator.

In this paper, a new quadrotor manipulation system is introduced. Two-link manipulator with two revolute joints is attached to the bottom of a quadrotor. The two axes of the revolute joints are perpendicular to each other. With this new system, the capability of manipulating objects with arbitrary location and orientation is enhanced because the degrees of freedom are increased from 4 to 6. On the other hand, the manipulator provides sufficient distance between the quadrotor and the object location. After modeling this new quadrotor manipulation system, a controller is designed based on feedback linearization technique in order to stabilize the system and provide satisfactory trajectory tracking.

The proposed system has a lot of potential applications such as:

- Demining applications/Improvised Explosive Device (IED) Disposal.
- Accessing payloads that are inaccessible to ground robots.
- Performing maintenance for a bridge or building.
- Hazardous material handling and removal.
- Removing obstacles that are blocking the view of a target or perch to conserve power.

This paper is organized as follows. The modeling of the proposed system is described in section II while section III introduces the controller design based on feedback linearization technique. The simulation results using MATLAB/SIMULINK are presented in section IV. Finally, main contributions are concluded in section V.

II. MODELING OF THE PROPOSED SYSTEM

In this section the equations of motion for quadrotor, manipulator and quadrotor-manipulator are discussed.

The structure of the proposed system is shown in Fig.1. The system consists of a two-link manipulator attached to the bottom of a quadrotor. The manipulator has two revolute

joints. The axis of joint 1 (z_0 in Fig.2) is parallel to one in-plane axis of the quadrotor (x in Fig.2) and perpendicular to the axis of joint 2. Also, the axis of joint 2 (z_1 in Fig.2) is parallel to the other in-plane axis of the quadrotor (y in Fig.2) at home (extended) configuration. Therefore the end effector can perform any arbitrary position and orientation. So, a 6–DOF aerial manipulator is obtained.

Joint 2 can be offset from joint 1 either along z_0-direction or along x_1-direction or along both directions. In Fig. 2, joint 2 is offset from joint 1 along z_0-direction which may give more freedom to position the end effector while the quadrotor is away from possible lateral obstacles.

The equations of motion of the quadrotor were driven in [2, 4, and 6].

A. System Kinematics

Fig. 2 presents a sketch of the quadrotor-manipulator system with the relevant frames. The orientation of the quadrotor is represented through Euler Angles.

A rigid body is completely described by its position and orientation with respect to a reference frame{E}, O_I- X Y Z that it is supposed to be earth-fixed and inertial. Let us define

$$R_I^B = \begin{bmatrix} \mathrm{C}(\psi)\mathrm{C}(\theta) & \mathrm{S}(\psi)\mathrm{C}(\theta) & -\mathrm{S}(\theta) \\ -\mathrm{S}(\psi)\mathrm{C}(\phi)+\mathrm{C}(\psi)\mathrm{S}(\theta)\,\mathrm{S}(\phi) & \mathrm{C}(\psi)\mathrm{C}(\phi)+\mathrm{S}(\psi)\mathrm{S}(\theta)\,\mathrm{S}(\phi) & \mathrm{C}(\theta)\mathrm{S}(\phi) \\ \mathrm{S}(\psi)\mathrm{S}(\phi)\mathrm{C}(\psi)\mathrm{S}(\theta)\mathrm{C}(\phi) & -\mathrm{C}(\psi)\,\mathrm{S}(\phi)+\mathrm{S}(\psi)\mathrm{S}(\theta)\mathrm{C}(\phi) & \mathrm{C}(\theta)\mathrm{C}(\phi) \end{bmatrix} \quad (1)$$

as the rotation matrix expressing the transformation from the inertial frame to the body-fixed frame{B}, O_b -x y z, where $\phi, \theta,$ and ψ are the body Euler-angle coordinates in an earth-fixed reference frame. These angles are commonly named roll, pitch and yaw angles and corresponds to the elementary rotation around X, Y and Z in fixed frame. The corresponding time derivatives of those angles are related to the body-fixed angular velocity components by a proper Jacobian matrix which can be expressed in terms of Euler angles as:

$$J = \begin{bmatrix} 1 & 0 & -\mathrm{S}(\theta) \\ 0 & \mathrm{C}(\phi) & \mathrm{C}(\theta)\,\mathrm{S}(\phi) \\ 0 & -\mathrm{S}(\theta) & \mathrm{C}(\theta)\,\mathrm{C}(\phi) \end{bmatrix} \quad (2)$$

where c(α) and s(α) are short notations for cos(α) and sin(α). The rotation R_I^B matrix is needed to transform the linear velocities.

In Fig. 2 the frames are assumed to satisfy the Denavit-Hartenberg convention [9]. Table I presents DH parameters for the 2-Link Manipulator. The position and orientation of the end-effector relative to the body-fixed frame is easily obtained by multiplying the following homogeneous transformation matrices:

$$A_0^B = \begin{bmatrix} 0 & 0 & 1 & 0 \\ 1 & 0 & 0 & 0 \\ 0 & 1 & 0 & -\mathrm{L}_0 \\ 0 & 0 & 0 & 1 \end{bmatrix} \quad (3)$$

$$A_1^0 = \begin{bmatrix} \mathrm{C}(\theta_1) & 0 & -\mathrm{S}(\theta_1) & 0 \\ \mathrm{S}(\theta_1) & 0 & \mathrm{C}(\theta_1) & 0 \\ 0 & -1 & 0 & -\mathrm{L}_1 \\ 0 & 0 & 0 & 1 \end{bmatrix} \quad (4)$$

where θ_1 and θ_2 are the manipulator joints' angles.

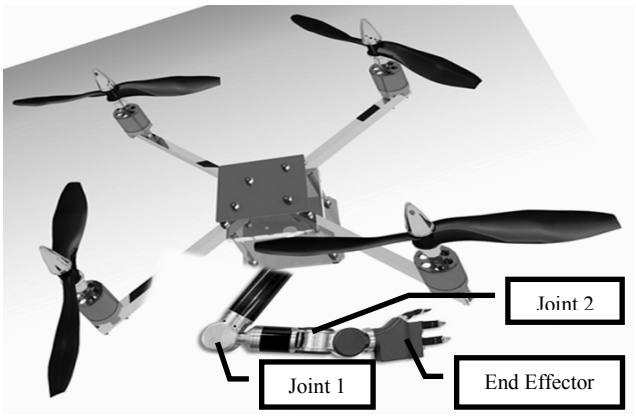

Figure 1. 3D model of the proposed system

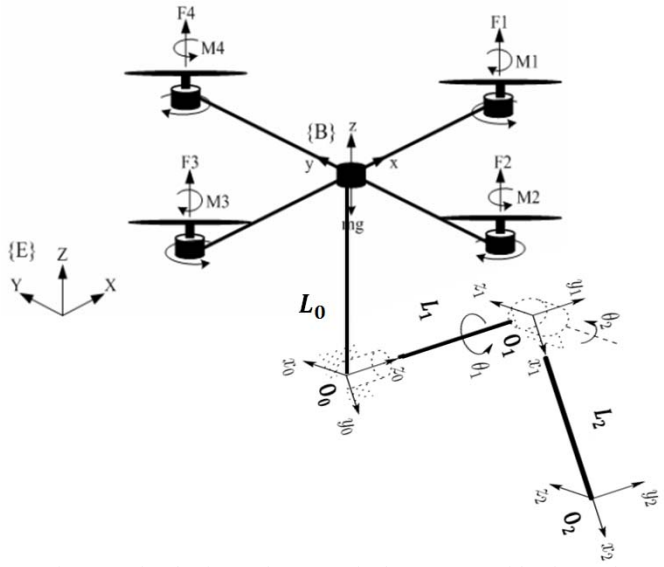

Figure 2. Sketch of a quadrotor-manipulator system with relevant frames

TABLE I. DH PARAMETERS FOR THE MANIPULATOR

Link	$\boldsymbol{d_i}$	$\boldsymbol{a_i}$	$\boldsymbol{\alpha_i}$	$_i$
0	$-L_0$	0	pi	pi
1	L_1	0	-pi	$_1$
2	0	L_2	0	$_2$

$$A_2^1 = \begin{bmatrix} \mathrm{C}(\theta_2) & -\mathrm{S}(\theta_2) & 0 & \mathrm{L}_2\mathrm{C}(\theta_2) \\ \mathrm{S}(\theta_2) & \mathrm{C}(\theta_2) & 0 & \mathrm{L}_2\mathrm{S}(\theta_2) \\ 0 & 0 & 1 & 0 \\ 0 & 0 & 0 & 1 \end{bmatrix} \quad (5)$$

Also, the position and orientation of the end effector relative to the inertial frame can be obtained by transforming its position and orientation from body frame to inertial frame by using R_B^I and the position vector expressed in the inertial frame.

B. System Dynamics

In Fig. 3, a block diagram that shows the effects of adding a manipulator to a quadrotor is presented.

For the manipulator dynamics, Recursive Newton Euler method [10] is used to derive the equations of motion. Since the quadrotor is considered to be the base of the manipulator,

the initial linear and angular velocities and accelerations, used in Newton Euler algorithm, are that of the quadrotor expressed in body frame. Applying the Newton Euler algorithm to the manipulator considering that the link (with length L_0) that is fixed to the quadrotor is the base link; equations (6) to (36) can be obtained. Let us define for each link i, the following variables: ω_i^i, angular velocity of frame i expressed in frame i, $\dot{\omega}_i^i$, angular acceleration of frame i, V_i^i, linear velocity of the origin of frame i, $\dot{V}_{ci}^i$, linear acceleration of the center of mass of link i, $\dot{V}_i^i$, linear acceleration of the origin of frame i, r_i^i , the vector from the origin of frame ($i-1$) to the center of mass of link i, , r_{ci}^i , the vector from the origin of frame $(i-1)$ to the center of mass of link i, g^I, the vector of gravity expressed in inertial frame I, z_{i-1}^{i-1}, is a unit vector pointing along the i^{th} joint axis and expressed in the (i-1)th link coordinate system, R_i^{i-1}, rotation matrix from frame i to frame i -1, I_i^i, the inertia matrix of link i about its center of mass coordinate frame. $f_{i,i-1}^i$/ $n_{i,i-1}^i$ are the resulting force/moment exerted on link i by link i -1 at point O_{i-1}, and i = 1, 2.

$$\omega_0^0 = R_B^0 v_2 \quad (6)$$

where v_2 is the body-fixed angular velocity.

$$\dot{\omega}_0^0 = R_B^0 \dot{v}_2 \quad (7)$$

$$r_0^0 = [0 \; -L_0 \; 0]^T \quad (8)$$

$$V_0^0 = R_B^0 v_1 + \omega_0^0 x r_0^0, \quad (9)$$

where v_1 is the body-fixed linear velocity.

$$\dot{V}_0^0 = R_B^0 \dot{v}_1 + \dot{\omega}_0^0 x r_0^0 + \omega_0^0 x (\omega_0^0 x r_0^0) \quad (10)$$

For links 1 and 2 (i = 1, 2) we calculate the following variables:

$$\omega_i^i = R_{i-1}^i (\omega_{i-1}^{i-1} + \dot{\theta}_i z_{i-1}^{i-1}) \quad (11)$$

$$\dot{\omega}_i^i = R_{i-1}^i (\dot{\omega}_{i-1}^{i-1} + z_{i-1}^{i-1} \ddot{\theta}_i + \omega_{i-1}^{i-1} x \dot{\theta}_i z_{i-1}^{i-1}) \quad (12)$$

$$V_i^i = R_{i-1}^i V_{i-1}^{i-1} + \omega_i^i x r_i^i \quad (13)$$

$$\dot{V}_i^i = R_{i-1}^i \dot{V}_{i-1}^{i-1} + \dot{\omega}_i^i x r_i^i + \omega_i^i x (\omega_i^i x r_i^i) \quad (14)$$

$$\dot{V}_{ci}^i = \dot{V}_i^i + \dot{\omega}_i^i x r_{ci}^i + \omega_i^i x (\omega_i^i x r_{ci}^i) \quad (15)$$

The inertial forces and moments acting on link i are given by:

$$F_i^i = -m_i \dot{V}_{ci}^i \quad (16)$$

$$n_i^i = -I_i^i \dot{\omega}_i^i - \omega_i^i x I_i^i \omega_i^i \quad (17)$$

The total forces and moments acting on link i are given by:

$$f_{i,i-1}^i = f_{i+1,i}^i - m_i g^i - F_i^i \quad (18)$$

$$n_{i,i-1}^i = n_{i+1,i}^i - m_i g^i + (r_i^i + r_{ci}^i) x f_{i,i-1}^i - r_{ci}^i x f_{i+1,i}^i - n_i^i \quad (19)$$

$$f_{i,i-1}^{i-1} = R_i^{i-1} f_{i,i-1}^i \quad (20)$$

$$n_{i,i-1}^{i-1} = R_i^{i-1} n_{i,i-1}^i \quad (21)$$

where,

$$z_0^0 = [0 \; 0 \; 1]^T, \quad (22)$$

$$r_1^1 = [0 \; -L_1 \; 0]^T, \quad (23)$$

$$r_{c1}^1 = [0 \; -L_1/2 \; 0]^T \quad (24)$$

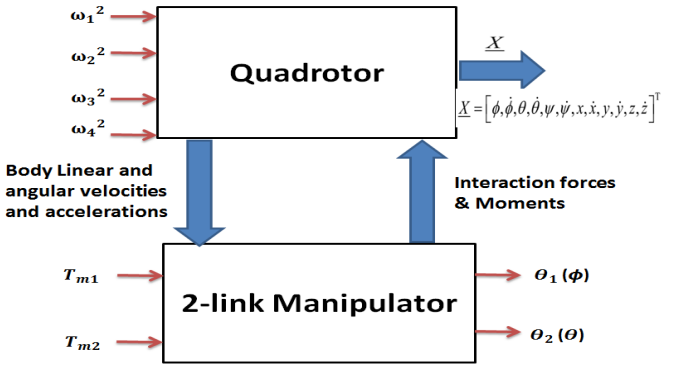

Figure 3. Effects of adding a manipulator to the quadrotor

$$z_1^1 = [0 \; 0 \; 1]^T, \quad (25)$$

$$r_2^2 = [L_2 \; 0 \; 0]^T, \quad (26)$$

$$r_{c2}^2 = [-L_2/2 \; 0 \; 0]^T. \quad (27)$$

The gravity vector expressed in frame 1 and 2 are:

$$g^I = [0 \; 0 \; -g]^T \quad (28)$$

$$g^2 = R_I^2 g^I \quad (29)$$

$$g^1 = R_I^1 g^I, \quad (30)$$

where,

(8)

$$R_I^1 = R_0^1 R_B^0 R_I^B \quad (31)$$

$$R_I^2 = R_1^2 R_I^1 \quad (32)$$

Let links 1 and 2 be square beams of relatively small cross-sectional area, then

$$I_i^i = \frac{m_i L_i^2}{12} \begin{bmatrix} 0 & 0 & 0 \\ 0 & 1 & 0 \\ 0 & 0 & 1 \end{bmatrix} \quad (33)$$

Where m_i and L_i are the mass and length of link i.

The external forces and moments acting on the end effector of the manipulator are assumed to be zeroes because in this paper, only position control of the system is considered:

$$f_{3,2}^2 = [0 \; 0 \; 0]^T \text{ and } n_{3,2}^2 = [0 \; 0 \; 0]^T, \quad (34)$$

The torques acting on joints 1 and 2 are finally given by:

$$T_{m1} = (n_{1,0}^0)^T z_0^0 + b_1 \dot{\theta}_1 \quad (35)$$

$$T_{m2} = (n_{2,1}^1)^T z_1^1 + b_2 \dot{\theta}_2 \quad (36)$$

where, b_1 and b_2 are friction coefficients.

The interaction forces and moments of the manipulator acting on the quadrotor expressed in body frame, $F_{m,q}^B$ and $M_{m,q}^B$ are given as follows:

$$P_{B0}^B = [0 \; 0 \; -L_0]^T \quad (37)$$

$$\begin{bmatrix} F_{m,q}^B \\ M_{m,q}^B \end{bmatrix} = \begin{bmatrix} R_0^B & O_{3x3} \\ \text{skew}(P_{B0}^B) R_0^B & R_0^B \end{bmatrix} \begin{bmatrix} f_{1,0}^0 \\ n_{1,0}^0 \end{bmatrix} \quad (38)$$

Where, skew (.) is skew symmetric matrix [9] of P_{B0}^B which is the position vector of the origin 0 relative to frame B.

The interaction forces expressed in inertial frame are:

$$F_{m,q}^I = R_B^I F_{m,q}^B \quad (39)$$

The equations of motion of the manipulator are:

$$M_1 \ddot{\theta}_1 = T_{m1} + N_1(\eta_2, \nu_2, \dot{\boldsymbol{\nu}}_2, \dot{\boldsymbol{\nu}}_1, \theta_1, \theta_2, \dot{\theta}_1, \dot{\theta}_2) \quad (40)$$

$$M_2 \ddot{\theta}_2 = T_{m2} + N_2(\eta_2, \nu_2, \dot{\boldsymbol{\nu}}_2, \dot{\boldsymbol{\nu}}_1, \theta_1, \theta_2, \dot{\theta}_1, \dot{\theta}_2), \quad (41)$$

Where, M_1, M_2, N_1, and N_2 are nonlinear terms.

The equations of motion of the quadrotor after adding the forces/moments applied by the manipulator are:

$$m\ddot{X} = T\,(C(\psi)\,S(\theta)\,C(\phi) + S(\psi)\,S(\phi)) + F^{I}_{m,q_x} \quad (42)$$

$$m\ddot{Y} = T\,(S(\psi)\,S(\theta)\,C(\phi) - C(\psi)\,S(\phi)) + F^{I}_{m,q_y} \quad (43)$$

$$m\ddot{Z} = -mg + T\,(C(\phi)\,C(\theta)) + F^{I}_{m,q_z} \quad (44)$$

$$I_x \ddot{\phi} = \dot{\theta}\dot{\psi}(I_y - I_z) - I_r \dot{\theta}\,\Omega + Ta_1 + M^{B}_{m,q_\phi} \quad (45)$$

$$I_y \ddot{\theta} = \dot{\phi}\dot{\psi}(I_z - I_x) + I_r \dot{\phi}\,\Omega + Ta_2 + M^{B}_{m,q_\theta} \quad (46)$$

$$I_z \ddot{\psi} = \dot{\phi}\dot{\theta}(I_x - I_y) + Ta_3 + M^{B}_{m,q_\psi} \quad (47)$$

The last three equations are derived, assuming that there are small variations in the three angles ϕ, θ and ψ such that the corresponding time derivatives of Euler angles are equivalent to the body-fixed angular velocities.

The variables in equations (42-47) are defined as follows:

T is the total thrust applied to the quadrotor from all four rotors, and is given by:

$$T = \sum_{j=1}^{4} F_j, \quad (48)$$

F_j is the thrust force from rotor j and is given by:

$$F_j = b\,\Omega_j^2, \quad (49)$$

Ω_j is the angular velocity of rotor j and b is the thrust coefficient.

Ta_1, Ta_2, and Ta_3 are the three moments about the three body axes, and are given as:

$$Ta_1 = d\,(F_4 - F_2) \quad (50)$$

$$Ta_2 = d\,(F_3 - F_1) \quad (51)$$

$$Ta_3 = K_d\,(-\Omega_1^2 + \Omega_2^2 - \Omega_3^2 + \Omega_4^2), \quad (52)$$

d is the distance between the quadrotor center of mass and the rotation axis of the propeller and K_d is the drag coefficient.

$$\Omega = \Omega_1 - \Omega_2 + \Omega_3 - \Omega_4 \quad (53)$$

I_r is the rotor inertia. I_f is the inertia matrix of the vehicle around its center of mass and assuming that the vehicle is symmetric about x, y and z, it is given by:

$$I_f = \begin{bmatrix} I_x & 0 & 0 \\ 0 & I_y & 0 \\ 0 & 0 & I_z \end{bmatrix} \quad (54)$$

III. Controller Design

This section discusses the control system design based on the technique of feedback linearization [8, 9]. Feedback linearization transforms the nonlinear system dynamics into a linear system. The control laws are chosen so that zero tracking errors are achieved [5].

Fig. 4 Presents a block diagram of the proposed control system, in order to stabilize the vehicle with the manipulator and to achieve a good position control for the movements in X, Y, Z, and ψ directions as well as for joints' angles θ_1 and θ_2.

A. Control Mixer.

The matrix G of the control mixer is used to transform the assigned thrust force and moments of the quadrotor (the control signals) from the controller block into assigned angular velocities of the four rotors.

This matrix can be derived from (48), (50), (51), and (52) and presented as following:

$$\begin{bmatrix} \Omega_1^2 \\ \Omega_2^2 \\ \Omega_3^2 \\ \Omega_4^2 \end{bmatrix} = \underbrace{\begin{bmatrix} b & b & b & b \\ 0 & -d\,b & 0 & d\,b \\ -d\,b & 0 & d\,b & 0 \\ -K_d & K_d & -K_d & K_d \end{bmatrix}^{-1}}_{G} \begin{bmatrix} T \\ Ta_1 \\ Ta_2 \\ Ta_3 \end{bmatrix} \quad (55)$$

B. Controller Block

Fig. 5 shows a block diagram describing what is inside the controller block of Fig. 4.

Quadrotor is an under-actuated system, because it has four inputs (angular velocities of its four rotors) and six variables to be controlled. By observing the operation of the quadrotor, one can find that the movement in x- direction is based on the pitch rotation, θ. Also the movement in y- direction is based on the roll rotation, ϕ.Therefore; X and Y will be controlled through controlling θ and ϕ respectively. Let us add subscript d to denote the desired variables. Taking into consideration the nonholonmic constraints of the system is of major importance. Nonholonomic constraints define the coupling between various states of the system. These nonholonmic constraints are used to determine the desired trajectories of θ and ϕ from the desired trajectories of X, Y, Z, ψ, θ_1, and θ_2. Then feedback linearization controllers are used to obtain a zero tracking errors for θ, ϕ, Z, ψ, θ_1 and θ_2.

C. Nonholonomic Constraints

From the equations of the translation dynamics (40-42), one can extract the expressions of the high-order nonholonmic constraints:

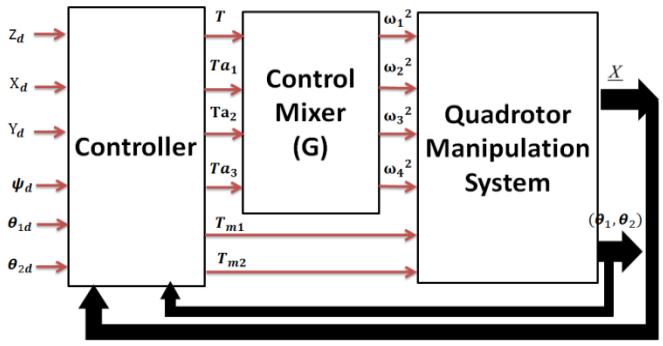

Figure 4. Block diagram of the proposed control system

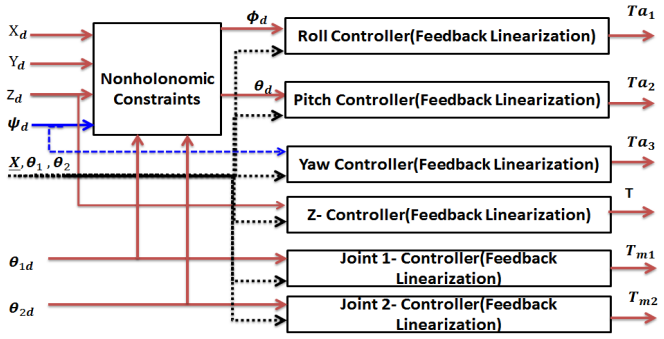

Figure 5. Block diagram of the controller block in Fig. 4

$$\sin(\phi) = \frac{(\ddot{X} - F^{I}_{m,q_x})\sin(\psi) - (\ddot{Y} - F^{I}_{m,q_y})\cos(\psi)}{\left((\ddot{X} - F^{I}_{m,q_x})^2 + (\ddot{Y} - F^{I}_{m,q_y})^2 + (\ddot{Z} + g - F^{I}_{m,q_z})^2\right)^{0.5}} \quad (56)$$

$$\tan(\theta) = \frac{(\ddot{X} - F^{I}_{m,q_x})\cos(\psi) + (\ddot{Y} - F^{I}_{m,q_y})\sin(\psi)}{\ddot{Z} + g - F^{I}_{m,q_z}} \quad (57)$$

where, F^{I}_{m,q_x}, F^{I}_{m,q_y} , F^{I}_{m,q_z} are functions of the system states and there derivatives.

Putting subscript d to all variables in (56) and (57), then ϕ_d and θ_d can be obtained.

D. Feedback Linearization

Z-Controller can be developed by expressing the equation of motion in z-direction in the following form

$$(m\ddot{Z} + mg - F^{I}_{m,q_z})/(C(\phi)\,C(\theta)) = T \quad (58)$$

The following control input will cancel out the nonlinearities in the system

$$T = (mU_z + mg - F^{I}_{m,q_z})/(C(\phi)\,C(\theta)) \quad (59)$$

Where,

$$U_z = \ddot{Z}_d + K_{pz}\,e_z + K_{dz}\,\dot{e_z} + K_{iz}\int_0^t e_z\,dt \quad (60)$$

The control law leads to the exponential stable dynamics

$$\ddot{e_z} + K_{dz}\,\dot{e_z} + K_{pz}\,e_z + K_{iz}\int_0^t e_z\,dt = 0 \quad (61)$$

which implies that $e_z \to 0$.

For ϕ, θ, ψ, θ_1 and θ_2 controllers a similar control laws are chosen

$$Ta_1 = I_x U_\phi - \dot{\theta}\dot{\psi}(I_y - I_z) + I_r\,\dot{\theta}\,\Omega - M^{B}_{m,q_\phi} \quad (62)$$

$$U_\phi = \ddot{\phi}_d + K_{p\phi}\,e_\phi + K_{d\phi}\,\dot{e_\phi} + K_{i\phi}\int_0^t e_\phi\,dt \quad (63)$$

$$Ta_2 = I_y U_\theta - \dot{\phi}\dot{\psi}(I_z - I_x) - I_r\,\dot{\phi}\,\Omega - M^{B}_{m,q_\theta} \quad (64)$$

$$U_\theta = \ddot{\theta}_d + K_{p\theta}\,e_\theta + K_{d\theta}\,\dot{e_\theta} + K_{i\theta}\int_0^t e_\theta\,dt \quad (65)$$

$$Ta_3 = I_z U_\psi - \dot{\phi}\dot{\theta}(I_x - I_y) - M^{B}_{m,q_\psi} \quad (66)$$

$$U_\psi = \ddot{\psi}_d + K_{p\psi}\,e_\psi + K_{d\psi}\,\dot{e_\psi} + K_{i\psi}\int_0^t e_\psi\,dt \quad (67)$$

$$T_{m1} = M_1 U_{\theta_1} - N_1 \quad (68)$$

$$U_{\theta_1} = \ddot{\theta}_{1d} + K_{p\theta_1}\,e_{\theta_1} + K_{d\theta_1}\,\dot{e_{\theta_1}} + K_{i\theta_1}\int_0^t e_{\theta_1}\,dt \quad (69)$$

$$T_{m2} = M_2 U_{\theta_2} - N_2 \quad (70)$$

$$U_{\theta_2} = \ddot{\theta}_{2d} + K_{p\theta_2}\,e_{\theta_2} + K_{d\theta_2}\,\dot{e_{\theta_2}} + K_{i\theta_2}\int_0^t e_{\theta_2}\,dt \quad (71)$$

where, K_p, K_d, K_i are the controller parameters.

IV. Simulation Results

The system equations of motions and the control laws are simulated using MATLAB/SIMULINK program.

Parameters of the system are listed in Table 2. The controller parameters are in Table 3. Quintic Polynomial Trajectories [8] are used as the reference trajectories for X, Y, Z, ψ, θ_1, and θ_2.Those types of trajectories have sinusoidal acceleration which is better in order to avoid vibrational modes. The desired trajectory for X-motion is shown in Fig. 6. Desired trajectories for Y, Z, ψ, θ_1 and θ_2 are the same as X-trajectory except for ψ, which has a final value of 0.1 (rad).

The tracking simulation results of desired trajectories along X, Y, Z, ψ, θ_1, and θ_2 are shown in Fig. 7.

TABLE II. SYSTEM PARAMETERS

Parameter	Value	Unit	Parameter	Value	Unit
b	2.9842×10^{-5}	N s^2	L_0	0.05	m
K_d	3.2320×10^{-7}	N m s^2	L_1	0.1	m
m	0.486	kg	L_2	0.2	m
d	0.25	m	m_0	0.010	kg
I_x	3.8278×10^{-3}	N m s^2	m_1	0.040	kg
I_y	3.8288×10^{-3}	N m s^2	m_2	0.070	kg
I_z	7.6566×10^{-3}	N m s^2	b_1	0.0	N/rad/s
I_r	2.8385×10^{-5}	N m s^2	b_2	0.0	N/rad/s
g	9.81	m /s^2			

TABLE III. CONTROLLERS PARAMETERS

Parameter	Value	Parameter	Value
[K_{pz} K_{dz} K_{iz}]	[16, 1, 8]	[$K_{p\psi}$ $K_{d\psi}$ $K_{i\psi}$]	[64, 6, 2]
[$K_{p\phi}$ $K_{d\phi}$ $K_{i\phi}$]	[64, 16, 1]	[$K_{p\theta_1}$ $K_{d\theta_1}$ $K_{i\theta_1}$]	[64, 16, 1]
[$K_{p\theta}$ $K_{d\theta}$ $K_{i\theta}$]	[115,0.01 , 0.01]	[$K_{p\theta_2}$ $K_{d\theta_2}$ $K_{i\theta_2}$]	[64, 16, 1]

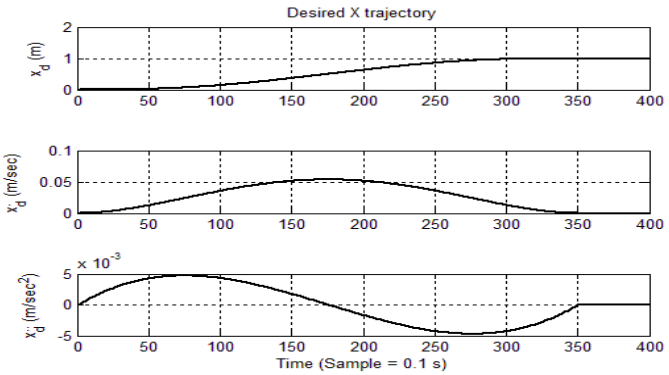

Figure 6. Desired X-trajectory

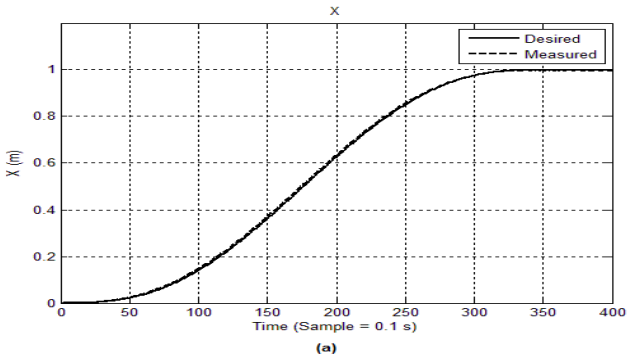

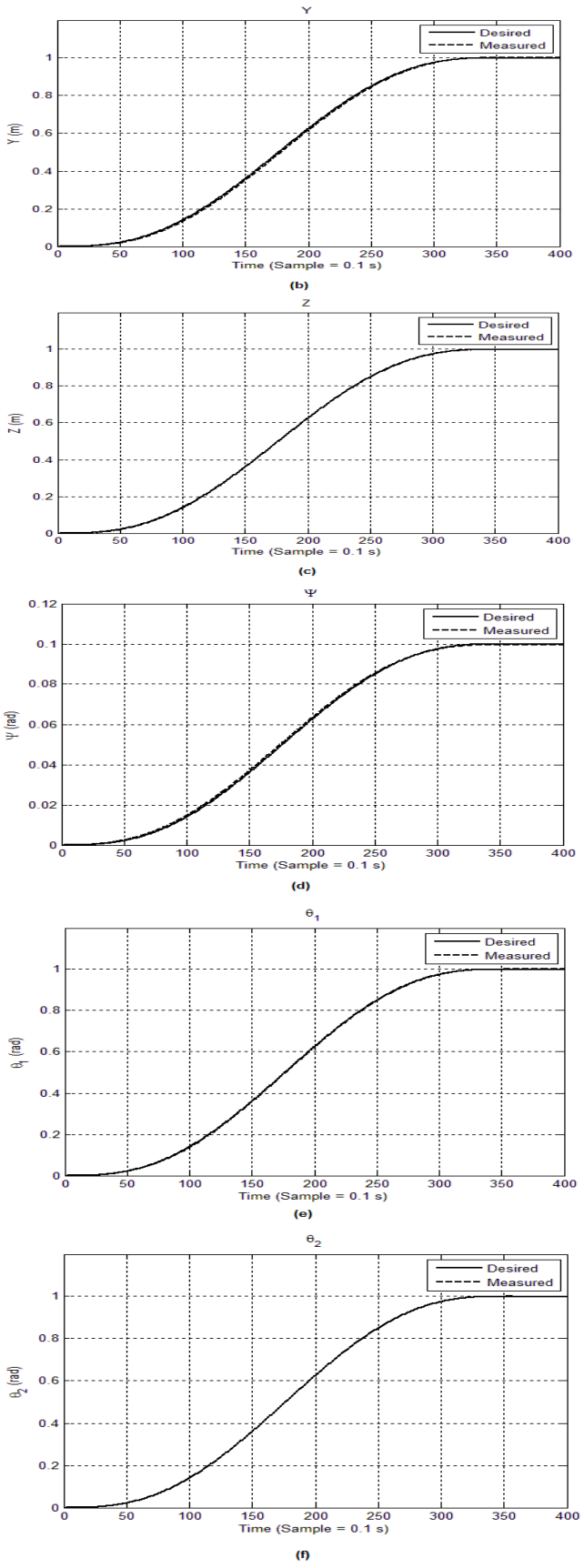

Figure 7. The Tracking simulation results of desired trajectories along (a) X-axis, (b) Y-axis, (c) Z-axis, (d) ψ - direction, (e) θ_1, and (f) θ_2.

V. CONCLUSION

In this paper, a new aerial manipulation system called "quadrotor manipulation system" was presented. This proposed system adds new features to the current aerial manipulation systems (quadrotor with a gripper) such that the end-effector becomes capable of arbitrary 6-DOF motion. The manipulator attached to the bottom of the quadrotor provides enough distance between the object to be manipulated and the quadrotor, which is desired in some applications. The detailed mathematical model for the quadrotor-manipulator system was presented. A controller was designed based on feedback linearization technique and the usage of the nonholonmic constraints. Quintic Polynomial Trajectories are used as the reference trajectories for X, Y, Z, ψ, θ_1 andθ_2. Simulations results show satisfactory tracking of the desired trajectories. As a future work, modeling and adaptive/robust control for this system after adding a payload to the end-effector will be considered. Also, experimental setup for the proposed system will be carried out.

ACKNOWLEDGMENT

The first author is supported by a scholarship from the Mission Department, Ministry of Higher Education of the Government of Egypt which is gratefully acknowledged.

REFERENCES

[1] D. Mellinger, Q. Lindsey, M. Shomin, and V. Kumar, "Design, Modeling, Estimation and Control for Aerial Grasping and Manipulation," IEEE/RSJ International Conference on Intelligent Robots and Systems San Francisco, CA, USA, September 25-30, 2011.

[2] J. Kim, M. Kang, S. Park, "Accurate Modeling and Robust Hovering Control for a Quad–rotor VTOL Aircraft," J Intell Robot Syst 2010.

[3] M. I. Rashid and S. Akhtar, "Adaptive Control of a Quadrotor with Unknown Model Parameters," 9th International Bhurban Conference on Applied Sciences &Technology (IBCAST)9th -12th January, 2012.

[4] H. Bouadi, and M. Tadjine, "Nonlinear Observer Design and Sliding Mode Control of Four Rotors Helicopter," WORLD ACADEMY OF SCIENCE, ENGINEERING AND TECHNOLOGY, 2007.

[5] I. Schjolberg and T. I. Fossen, "Modelling and Control of Underwater Vehicle-Manipulator Systems ," in Proc. rd Conf. on Marine Craft maneuvering and control, 1994.

[6] T. Bresciani, Modelling, Identification and Control of a Quadrotor Helicopter. MSc thesis, Lund University,October 2008.

[7] S. Bouabdallah. Design and Control of Quadrotors with Application to Autonomous Flying. PhD thesis, Ecole Polytechnique Federale , 2007.

[8] J.-J. E. SLOTINE and W. LI, Applied Nonlinear Control, Prentice-Hall, 1991, pp. 207-266.

[9] M. W. Spong, S. Hutchinson, and M. Vidyasagar, Robot Modeling and Control, 1st ed, JOHN WILEY & SONS,2005, pp. 65-75, pp. 113-120, pp. 173-182, pp. 207-266, pp. 315-317.

[10] L.-W. Tsai, ROBOT ANALYSIS: The Mechanics of Serial and Parallel manipulators, JOHN WILEY&SONS, 1999, pp. 275-278, pp. 372-410.